The Cellular Prion Protein Controls Notch Signaling in Neural Stem/Progenitor Cells

Séverine Martin-Lannerée, Sophie Halliez, Théo Z Hirsch, Julia Hernandez-Rapp, Bruno Passet, Céline Tomkiewicz, Ana Villa-Diaz, Juan-Maria Torres, Jean-Marie Launay, Vincent Béringue, et al.

Running head: PrP controls Notch in neural stem/progenitor cells

The Cellular Prion Protein Controls Notch Signalling in Neural Stem / Progenitor Cells

Séverine Martin-Lannerée,[1,2] Sophie Halliez,[3,8,†] Théo Z. Hirsch,[1,2,†] Julia Hernandez-Rapp[1,2,9], Bruno Passet[4], Céline Tomkiewicz,[1,2] Ana Villa-Diaz[5], Juan-Maria Torres[5], Jean-Marie Launay[6,7], Vincent Béringue[3], Jean-Luc Vilotte[4] & Sophie Mouillet-Richard[1,2,*]

[1] INSERM UMR 1124, 75006 Paris France.

[2] Université Paris Descartes, Sorbonne Paris Cité, UMR 1124, 75006 Paris France.

[3] VIM, INRA, Université Paris-Saclay, 78350, Jouy-en-Josas, France

[4] INRA UMR1313, Génétique animale et biologie intégrative, 78350 Jouy-en-Josas, France

[5] Centro de Investigación en Sanidad Animal-INIA, 28130 Madrid, Spain

[6] AP-HP Service de Biochimie, Fondation FondaMental, INSERM U942 Hôpital Lariboisière, 75010 Paris, France

[7] Pharma Research Department, F. Hoffmann-La-Roche Ltd., CH-4070 Basel, Switzerland.

[8] Present address: CNRS UMR7592, Jacques Monod Institute, 75205 Paris Cedex 13, France

[9] Present address: Centre de recherche du CHU de Québec, Université Laval, Québec, G1V4G2 Québec, Canada

† Sophie Halliez and Théo Z. Hirsch contributed equally to this work.

Contributions: S.M.L.: conception and design, collection and assembly of data, data analysis and interpretation, manuscript writing and final approval of the manuscript; S.H., T.Z.H., J.H.R., B.P. and C.T.R.: collection and assembly of data, data analysis and interpretation and final approval of the manuscript; A.V.D.: provision of study material; J.M.T.: provision of study material and final approval of the manuscript; V.B., J.L.V. and J.M.L.: data analysis and interpretation and final approval of the manuscript; S.M.R.: conception and design, financial support, data analysis and interpretation, manuscript writing and final approval of the manuscript.

* Correspondence: Sophie Mouillet-Richard, PhD, INSERM UMR 1124, Université Paris Descartes, 45 rue des Saints-Pères, 75006 Paris, France, Telephone: 33-1-42-86-42-40. Fax: 33-1-42-86-38-68. Email: sophie.mouillet-richard@parisdescartes.fr

Keywords: prion protein; Notch; neural stem cells; EGFR; cadherins

ABSTRACT

The prion protein is infamous for its involvement in a group of neurodegenerative diseases known as Transmissible Spongiform Encephalopathies. In the longstanding quest to decipher the physiological function of its cellular isoform, PrP^C, the discovery of its participation to the self-renewal of hematopoietic and neural stem cells has cast a new spotlight on its potential role in stem cell biology. However, still little is known on the cellular and molecular mechanisms at play. Here, by combining *in vitro* and *in vivo* murine models of PrP^C depletion, we establish that PrP^C deficiency severely affects the Notch pathway, which plays a major role in neural stem cell maintenance. We document that the absence of PrP^C in a neuroepithelial cell line or in primary neurospheres is associated with drastically reduced expression of Notch ligands and receptors, resulting in decreased levels of Notch target genes. Similar alterations of the Notch pathway are recovered in the neuroepithelium of *Prnp*$^{-/-}$ embryos during a developmental window encompassing neural tube closure. In addition, in line with Notch defects, our data show that the absence of PrP^C results in altered expression of Nestin and Olig2 as well as N-cadherin distribution. We further provide evidence that PrP^C controls the expression of the epidermal growth factor receptor (EGFR) downstream from Notch. Finally, we unveil a negative feedback action of EGFR on both Notch and PrP^C. As a whole, our study delineates a molecular scenario through which PrP^C takes part to the self-renewal of neural stem and progenitor cells.

INTRODUCTION

The cellular prion protein PrP^C is a highly conserved, ubiquitous glycoprotein that is mainly studied for its involvement in a group of neurodegenerative disorders known as Transmissible Spongiform Encephalopathies [1]. It is mostly found at the cell surface, where it may interact with a great diversity of partners, from extracellular matrix components to soluble ligands such as the extracellular chaperone stress-inducible 1 (STI-1) protein [2]. Over the past decade, PrP^C has emerged as a key actor of stem cell proliferation and/or self renewal [3, 4]. It was first identified as a cell-surface marker for hematopoietic stem cells (HSCs), and shown to sustain the long-term repopulating activity of HSCs [5]. It was also found to positively regulate neural precursor cell proliferation, in accordance with its abundant expression in the developing and adult central nervous system (CNS) [6]. In line with this, the interaction of PrP^C with STI-1 was shown to enhance the self-renewal of neural progenitors [7]. PrP^C has also been depicted as a marker for mammary stem cells [8] and cardioprogenitors [9]. Further, we [10] and others [11] have shown that PrP^C is upregulated following the cell fate restriction of pluripotent embryonic stem (ES) or carcinoma (EC) cells towards the neuronal lineage. Finally, we recently documented an enrichment of PrP^C at the base of the primary cilium in stem and progenitor cells from the CNS and cardiovascular system of developing embryos [12]. Collectively, these data support the notion that PrP^C is involved in stem cell homeostasis, but its specific contribution to stem cell proliferation, maintenance in an undifferentiated state, choice of cell fate or ability to enter a differentiation program remains incompletely understood.

The present work aims at delineating the contribution of PrP^C to neuroepithelial stem cell homeostasis by combining a synergy of *in vitro* and *in vivo* analyses. Our *in vitro* experiments exploit the EC-derived murine 1C11 neuroepithelial cell line [13], endogenously expressing PrP^C [10, 14], and its stably PrP^C-depleted derivatives (PrP^{KD}-1C11 cells) [15], as well as

primary neurospheres from WT and *Prnp*$^{-/-}$ mice [16]. In 1C11 cells, shRNA-mediated silencing of PrP^{C} severely affects the Hedgehog pathway [12], which plays an overriding role in neural stem cells [17].

Here, we found that PrP^{C} silencing drastically impacts on Notch signalling, a critical pathway involved in stem cell maintenance [18], by hindering the expression of the Notch ligands Jagged1 and Jagged2 as well as that of Notch receptors. The *in vivo* relevance of these results is substantiated by our analyses on *Prnp*$^{-/-}$ mice embryos revealing defects in the Notch pathway slightly after the onset of PrP^{C} expression in the neural folds. Furthermore, our data highlight various outcomes of PrP^{C} depletion downstream from Notch, including alterations in neural stem cell markers, cell architecture and, most notably, expression of the epidermal growth factor receptor (EGFR), whose activation exerts a negative feedback action on the Notch pathway as well as PrP^{C} expression.

MATERIALS AND METHODS

Animals

Animal experiments were carried out in strict accordance with the recommendations in the guidelines of the Code for Methods and Welfare Considerations in Behavioural Research with Animals (Directive 86/609EC) and all efforts were made to minimize suffering. Experiments were approved by the Local Ethics Committee of Jouy-en-Josas (Comethea, Permit number 12-034). E8.5 to E10.5 FVB/N (WT) and FVB/N *Prnp*$^{-/-}$ [19] mouse embryos from, respectively, WT x WT and *Prnp*$^{-/-}$ x *Prnp*$^{-/-}$ crossings were dissected in ice cold PBS and immediately frozen in liquid nitrogen for RNA analysis or fixed for immunofluorescence analyses.

Cell Culture and Treatments

1C11 cells and their PrP-KD counterparts were grown as in [15]. For cells grown on Jagged1, culture dishes were pre-coated with recombinant Jagged1-Fc at 3µg/cm^2 or control IgG1-Fc in PBS. Mouse neurospheres were obtained by whole brain dissection of E14 embryo from two lines from the same 129/ola strain: wild-type and *Prnp*$^{-/-}$ mice homozygous for a targeted null mutation in the *Prnp* gene [20]. Cells were grown as previously described in [16], i.e. in the presence of 20ng/ml EGF and 20ng/ml bFGF.

Immunofluorescence, Western Analysis and Quantitative Real-Time PCR

Detailed methods are presented in Supporting Information Materials and Methods.

Statistics

The results are reported as the means ± standard errors of the means (s.e.m.). The unpaired Student's *t*-test and the paired Wilcoxon's test were used for comparisons. A p-value < 0.05 was considered significant.

RESULTS

PrP^C depletion in neural stem / progenitor cells cancels the expression of Notch pathway effectors and switches off Notch signalling

To assess the contribution of PrP^C to neural stem cell homeostasis, we first analyzed the impact of the absence of PrP^C on the status of the Notch pathway, which plays a critical role in neural stem cell maintenance [18]. Activation of Notch transmembrane receptors induces the proteolytic cleavage of the Notch protein and nuclear translocation of its intracellular domain (Notch ICD, NICD), which interacts with the DNA-binding protein CBF1 to induce the transcription of target genes [18]. We first exploited the 1C11 cell line, in which we had previously documented a nuclear staining with anti-Notch polyclonal antibodies, indicating an activation of the Notch pathway [13]. The Notch nuclear staining was consistently observed in 1C11 cells, but was not recovered in their PrP-KD counterparts (Supporting Information Fig. S1), indicating that PrP^C knockdown in 1C11 cells switches off the Notch pathway. In line with this, the level of transcripts encoding the Notch target gene *Hes1* in PrP-KD cells was only 30% of that found in the parental 1C11 cells, as measured through quantitative PCR (qRT-PCR) (Fig. 1A). We went on to analyze the expression of mRNAs encoding the Notch receptors and their ligands Jagged1 (*Jag1*) and Jagged2 (*Jag2*) in 1C11 cells and their PrP-KD derivatives. We monitored strong reductions in the mRNA levels of *Jag1* and *Jag2* (16% and 22% vs. control, respectively) (Fig. 1B) as well as *Notch1* (20% vs. control) (Fig. 1C) when PrP^C was knocked-down in 1C11 cells. The amount of transcripts encoding *Notch2* were slightly but significantly lower in PrP^{KD}-1C11 cells versus their parental 1C11 cells, while *Notch3* transcripts were upregulated by 40% (Fig. 1C). *Notch4* mRNAs were barely detected, irrespective of PrP^C expression (data not shown).

To potentially extend these findings to another paradigm of PrP^C depletion, we compared the status of the Notch pathway in neurospheres (NSC) derived from *Prnp*$^{-/-}$ vs. WT embryos

[16]. Of note, we first confirmed the negative impact of PrP^{C} depletion on the activity of the Notch pathway since *Hes1* mRNA was significantly decreased (66% vs. control) in *Prnp*$^{-/-}$ NSC (Fig. 1D). Similarly to PrP^{KD}-1C11 cells, *Prnp*$^{-/-}$ NSC also exhibited reduced levels of *Jag1* and *Jag2* mRNAs (35% and 19% vs. control, respectively) (Fig. 1E). In this case, however, we found a milder reduction in the transcripts encoding *Notch1*, together with a strong decrease in *Notch3* mRNAs (19% vs. control) (Fig. 1F).

At the protein level, we confirmed the downregulation of Jagged1 (16 % and 58% vs. control) (Fig. 1G, 1I) in both PrP^{C}-depleted 1C11 cells and NSC, respectively, while the expression of Jagged2 could not be examined in western blot due to the lack of appropriate antibody. We further monitored reduced protein expression levels of Notch1 (21 % and 27% vs. control) (Fig. 1H, 1J) in PrP^{KD}-1C11 cells and *Prnp*$^{-/-}$ NSC, respectively. Altogether, these observations indicate that the absence of PrP^{C} in 1C11 cells or NSC blunts the expression of Jagged1 and Jagged2 as well as Notch1 and /or Notch3 and obliterates Notch signalling, as mirrored by the reduction in *Hes1* mRNA.

PrP^{C} depletion *in vivo* is associated with defects in Notch signalling at early embryonic stages

To assess the *in vivo* relevance of our *in vitro* findings, we analysed the expression of *Jag1*, *Jag2*, *Notch1*, *Notch2*, and *Notch3* through qRT-PCR in *Prnp*$^{-/-}$ versus WT mice at early embryonic stages. We also selected two Notch target genes for analysis: *Hes5* and the brain lipid binding protein (*Blbp*), whose expression in the developing nervous system correlates with Notch activity and defines neural stem and progenitor cells *in vivo* [21, 22]. We chose to start our analyses at embryonic day (E) 8.5, just after the detection of *Prnp* expression in the neural folds (E8.0) [23]. *Prnp*$^{-/-}$ E8.5 embryos exhibited similar level of *Jag1* but strongly reduced level of *Jag2* compared to their WT counterparts (46% vs. WT) (Supporting

Information Fig. S2A). In contrast, PrP^C invalidation was associated with mild but significant increases in *Notch1* and *Notch2* mRNAs (130% and 117% vs. WT, respectively) (Supporting Information Fig. S2B). This may reflect Notch expression in tissues other than the developing nervous system [24]. The marked decrease in *Blbp* transcripts in *Prnp*$^{-/-}$ embryos (18% vs. WT) (Supporting Information Fig. S2C) is, however, consistent with an alteration of Notch signalling in the developing nervous system [22].

We next sought to refine our study focusing on the developing CNS by performing analyses on dissected neural tube samples, which can be prepared from E9 onwards. In E9 neural tubes, we confirmed an alteration of the Notch pathway in a PrP-null context with a significant decrease in the expression of *Jag2* and most notably *Hes5* and *Blbp* (81%, 75% and 33% vs. WT, respectively) (Supporting Information Fig. S2D, S2F). There was also a trend towards reduced *Notch1* level in the absence of PrP^C although not statistically significant (Supporting Information Fig. S2E). In *Prnp*$^{-/-}$ neural tubes corresponding to E9.5, i.e. at the completion of cranial fold and caudal neuropore closure, the alteration of the Notch pathway was more prominent with significant reductions in *Jag1*, *Jag2*, *Notch1* and *Notch3* mRNAs (83%, 71%, 75% and 80% vs. WT, respectively) (Fig. 2A, 2B). To the opposite, *Notch2* expression was very slightly but significantly increased (112% vs. WT) (Fig. 2B). The decrease in the mRNA levels of *Hes5* and *Blbp* was further amplified at this stage (62% and 29% vs. WT, respectively) (Fig. 2C), revealing defective Notch signalling in the absence of PrP^C. In neural tubes from E10.5 embryos, most of these changes vanished or even reversed, with slight but significant increases in *Jag1* and *Notch1* levels (Fig. 2F, 2G). In contrast, the decrease in *Blbp* expression persisted, although less pronounced than in E9.5 neural tubes (56% vs. WT) (Fig. 2H).

As a whole, these results indicate that, as observed *in vitro*, the absence of PrP^C *in vivo* is associated with a downregulation of the Notch pathway starting around E8.5. Importantly,

this alteration is observed within a narrow time-window only and is the most apparent in neural tubes from E9.5 embryos, i.e. at a stage corresponding to full neural tube closure, when the neuroepithelium is highly proliferative [25]. Further, the decrease in transcripts encoding Hes5 and BLBP, two markers of neuroepithelial and radial glial progenitors [21, 22], mirrors a reduction in the pool of neural stem / progenitor cells in the absence of PrP^C.

Prnp$^{-/-}$ early embryos show alterations in neural stem cell identity markers

In view of the well-established control exerted by the Notch pathway on neural cell fate, we went on to analyze the expression of the stem cell markers Sox2, Nestin and Pax6 in neural tubes from *Prnp*$^{-/-}$ versus WT embryos. At E9.5, both *Sox2* and *Nestin* mRNAs were reduced in the absence of PrP^C (Fig. 2D). The decrease in *Nestin* expression was still apparent at E10.5 (Fig. 2I), while no significant difference was observed for *Pax6* at either stage (Fig. 2D, 2I). Finally, it is now acknowledged that Notch activity in the neural tube contributes to the specification of the most ventral so-called p3 domain and that defective Notch signalling is associated with an expansion of the adjacent, less ventral domain known as pMN (which gives rise to motor neurons and is marked by the expression of Olig2) at the expense of the p3 domain, while increased Notch signalling has opposite effects [26]. In line with this, NICD was shown to negatively regulate the expression of Olig2 in glioma stem cells [27]. In accordance with the above alterations in the Notch pathway in neural tubes from *Prnp*-ablated mouse embryos, we monitored a two-fold increase in the expression of *Olig2* in *Prnp*$^{-/-}$ vs. WT neural tubes at E10.5 (Fig. 2J). In contrast, transcripts encoding PDGFRα, a marker of oligodendrocyte progenitor cells [28], were insensitive to *Prnp* ablation (Fig. 2J).

We went on to examine the pattern of Nestin distribution in the neural tubes from E9.5 and E10.5 *Prnp*$^{-/-}$ vs. WT embryos by immunostaining of transverse sections of the neural tube. In WT embryos, Nestin exhibits a regular staining of fibres extending from the ventricular zone

to the mantle zone (Fig. 3A, left panels). At E9.5, Nestin staining appeared less organized in *Prnp*$^{-/-}$ embryos, especially across the neural tube and near the mantle zone in the presumptive hindbrain region (Fig. 3A, top right panels) as well as in the trunk region (Fig. 3A, bottom right panels). These differences were mitigated at E10.5 (Supporting Information Fig. S3, bottom panels). We then compared the distribution of the proliferation marker Ki67 between *Prnp*$^{-/-}$ and WT embryos. At E9.5, Ki67 staining was less regular in *Prnp*$^{-/-}$ vs. WT embryos (Supporting Information Fig. S4). At E10.5, this effect was more pronounced, notably in the ventral part of the neural tube, with regions devoid of Ki67^{+} cells (Fig. 3B, compare right versus left panels, see arrow). These observations suggest reduced neural stem cell proliferation in the absence of PrP^{C}. Finally, we found a slight but significant (123%, $p<0.05$, Wilcoxon's test) extension of the Olig2-positive zone in the mid-trunk region of *Prnp*$^{-/-}$ versus WT embryos at E10.5 (Fig. 3C), which is no longer visible at E11.5 (data not shown).

Thus, the defects in Notch signalling recorded in early *Prnp*$^{-/-}$ embryos are accompanied by changes in the expression of defined neural stem identity markers, with apparent - albeit subtle - alterations in neural tube patterning.

PrP^{C} depletion in 1C11 cells affects N-cadherin dependent cell-cell contacts

In the developing CNS, neural stem cells and their progenies form a highly structured epithelial tissue, whose architecture is notably regulated through N-cadherin-based intercellular contacts [29]. N-cadherin contributes to the regulation of the balance between self-renewal and differentiation [29] and the disruption of adherens junction integrity is associated with premature differentiation of neural stem cells [30]. To get insight into the impact of PrP^{C} knockdown on the architecture of 1C11 cells, we carried out immunofluorescence experiments to assess the distribution of N-cadherin as well as β-catenin, which associates with the intracellular domain of cadherins at the adherens junction.

1C11 cells form an epithelium and both N-cadherin and β-catenin were evenly distributed at the membrane, lining cell-cell contacts (Fig. 4A). In contrast, these contacts were strongly reduced in PrP^{C}-depleted cells. In line with this, both N-cadherin and β-catenin membrane stainings were markedly affected (Fig. 4A). Similar alterations were found in 1C11 cells 48h after transfection with two distinct PrP^{C}-targeting siRNAs (see Supporting Information Fig. S5, S6, S7). Changes monitored in PrP^{KD}-1C11 cells correlated with an increase in N-cadherin mRNA (*N-cad*) (184% vs. control) (Supporting Information Fig. S8A) and protein (158% vs. control) (Fig. 4B) levels in PrP^{C} depleted cells. Finally, while the expression of β-catenin mRNA *(ß-cat*) was not statistically different (Supporting Information Fig. S8A), we monitored a significant decrease at the protein level in PrP^{KD}-1C11 cells (60 % vs. control) (Fig. 4B). This observation is consistent with reduced stabilization of β-catenin due to decreased N-cadherin-mediated cell adhesion [31].

Altogether, these data indicate that PrP^{C} deficiency in the 1C11 neuroprogenitor promotes a drastic reduction of intercellular contacts mediated by N-cadherin, as well as a decrease of β-catenin level.

Prnp$^{-/-}$ early embryos exhibit N-cadherin patterning alterations

In view of the alterations of N-cadherin expression and staining in PrP^{KD}-1C11 cells, we then compared its expression in neural tubes from WT and *Prnp*$^{-/-}$ embryos at E9, E9.5 and E10.5. Whatever the developmental stage analyzed, we found similar *N-cad* mRNA levels in *Prnp*$^{-/-}$ and WT mice (Supporting Information Fig. S8B). Next, we examined the pattern of N-cadherin in *Prnp*$^{-/-}$ and WT embryos at E8.5 and E9.5 by immunostaining of transverse sections of the neural tube in the presumptive hindbrain and mid-trunk regions. At E8.5 in the presumptive mid-trunk region, while the pattern of N-cadherin staining in WT embryos was mainly localized to the apical face of the neuroepithelium (i.e. the ventricular zone, where

neural stem cells reside), it appeared to extend towards the external part of the neuroepithelium (i.e. the mantle zone) in *Prnp*$^{-/-}$ embryos (Supporting Information Fig. S9). At E9.5, the difference in N-cadherin staining persisted in a fraction (n=2 out of 3) of the *Prnp*$^{-/-}$ embryos, most notably in the caudal trunk region (Fig. 4C). When we measured the relative distribution of N-cadherin staining along the thickness of the neural tube in the caudal trunk region, from the apical face to the mantle zone, we found that the profile of N-cadherin distribution was very similar among WT embryos, with a peak in intensity in the apical-most part of the neural tube (Fig. 4D). While this peak in intensity is still present in the apical-most part of the neural tube in *Prnp*$^{-/-}$ embryos, we observed that 2 out of 3 *Prnp*$^{-/-}$ embryos exhibited shifted N-cadherin distribution towards the mantle zone (Fig. 4E).

These data argue for subtle but consistent alterations in N-cadherin distribution in the neural tube of *Prnp*$^{-/-}$ embryos, which, interestingly, are reminiscent of those observed in the spinal cord after transfection with a dominant negative form of N-cadherin [30].

Intact Jagged-Notch mediated signalling is necessary for the maintenance of cell-cell contacts

Having shown that PrP^{C} depletion disrupts cell architecture and affects Notch signalling, we probed the occurrence of a causal relationship between the two sets of alterations. To this purpose, we sought to restore the Jagged-Notch cascade in PrP^{KD}-1C11 cells by growing the cells on dishes coated with Jagged1 for 24h. With Jagged1, we observed a robust (369% vs. control) increase in transcripts encoding the Notch target gene *Hes1*, indicating that the Notch pathway is indeed turned on (Fig. 5C). In these conditions, *Hes1* mRNAs reached similar levels as those monitored in the parental 1C11 cells (data not shown). This treatment actually boosted the expression of *Jag1*, *Jag2* and *Notch1* (216%, 179% and 175% vs. controls, respectively) (Fig. 5A, 5B), highlighting a positive autoregulatory loop induced by Jagged1,

as reported in the literature [32, 33]. We next examined N-cadherin expression and found no variation at the mRNA level (Fig. 5D), but an increased protein level (138 % vs. control) in PrP^{KD}-1C11 cells exposed to Jagged1 (Fig. 5E). In immunofluorescence experiments, we observed a strengthening of cellular contacts, which were regularly stained with anti-N-cadherin antibodies, suggesting the establishment of N-cadherin-dependent cell-cell interactions in PrP^{C}-depleted cells upon rescue of the Notch pathway (Fig. 5F). We finally analyzed the distribution of β-catenin, which is expected to be retained at the plasma membrane upon cadherin-mediated adhesion. Antibodies against β-catenin indeed yielded an even submembrane staining in Jagged-treated PrP^{KD}-1C11 cells (Fig. 5F). Altogether, these data indicate that the restoration of an active Notch pathway in PrP-deficient cells rescues N-cadherin-mediated cell adhesion.

PrP^{C} controls the expression of EGFR via Notch

We finally sought to assess the impact of PrP^{C} depletion on a third protagonist, EGFR, which is known to modulate the proliferation, migration and fate of neural progenitors during embryonic development [34, 35]. EGFR was identified as a direct Notch target gene in adult neural stem cells [36], and its interaction with the Notch pathway regulates adult neural stem cell self-renewal [37]. We found a decrease in the expression of EGFR in PrP^{KD}-1C11 cells as compared to their parental 1C11 cells at both the mRNA and protein levels (57% and 55 % vs. control) (Fig. 6A, 6B). A similar impact of PrP^{C} depletion on EGFR expression was observed in *Prnp*$^{-/-}$ NSC (Fig. 6C, 6D), as well as *in vivo* in neural tubes samples from *Prnp*$^{-/-}$ mice at E9 and E9.5 (Fig. 6E). The decrease in *Egfr* transcripts persisted at E10.5, with levels reaching only 55% of control (Fig. 6E). Thus, the downregulation of *Egfr* monitored in the developing CNS in *Prnp*$^{-/-}$ animals correlated with the alteration of Notch activity (see Fig. 2).

Next, we found an upregulation of EGFR mRNA (167% vs. control) and protein (237 % vs. control) in PrP^{KD}-1C11 cells exposed to Jagged1 (Fig. 6F, 6G). Altogether, these data indicate that the absence of PrP^{C} *in vitro* and *in vivo* affects the expression of EGFR and provide evidence for an involvement of the Notch pathway in this regulation.

EGFR exerts a reciprocal negative control on Notch and PrP^{C}

In our last set of experiments, we sought to delineate how EGFR may participate to the stem cell properties of 1C11 cells, in relation with PrP^{C}. To this purpose, 1C11 cells were exposed to EGF (10ng/ml, 24h) and further analysed for the status of the Notch pathway as well as for PrP^{C} expression through qRT-PCR. We found a clear-cut negative effect of EGF on the Notch pathway, with significant reductions in the expression of *Jag1* (59% vs. control) (Fig. 7A), *Notch1* and *Notch3* (76% and 68% vs. control, respectively) (Fig. 7B) as well as *Hes1* and *Blbp* (76% and 31% vs. control, respectively) (Fig. 7C). There was also a trend towards reduced *Jag2* mRNAs, although not statistically significant (Fig. 7A). In contrast, *Notch2* mRNAs were unaffected by EGF (Fig. 7B). Interestingly, EGF also promoted a reduction in the expression of the PrP^{C}-encoding *Prnp* transcripts (76% vs. control) (Fig. 7D). The EGF-dependent downregulation of PrP^{C} was confirmed at the protein level (76 % vs. control) (Fig. 7E). Thus, EGFR activation appears to act as a brake on both the Notch pathway and PrP^{C} expression.

Then, to mimic the neurogenic stem cell niche [38], we sought to boost the Notch pathway by growing 1C11 cells on Jagged1-coated dishes. As observed with PrP^{KD}-1C11 cells, this treatment promoted a strong increase in the expression of various key components of the Notch pathway itself: *Jag1* and *Jag2* (290% and 280% vs. controls, respectively) (Fig. 7F), *Notch1* and *Notch3* (225% and 220% vs. controls, respectively) (Fig. 7G), *Hes1* and *Blbp* (225% and 860% vs. controls, respectively) (Fig. 7H). In line with data obtained with PrP^{KD}-

1C11 cells upon restoration of an active Notch pathway, *Egfr* mRNA level was also upregulated in Jagged1-treated 1C11 cells (195% vs. control) (Fig. 7I). Of note, the expression of *Prnp* was also modestly but significantly increased in these conditions (129% vs. control) (Fig. 7J). Finally, in view of the crosstalk interactions between Notch and EGFR signalling in various paradigms [39, 40] and most notably in the regulation of adult neural stem cell self-renewal [37], we examined the impact of combined exposure of 1C11 cells to Jagged1 and EGF on the same target genes. Interestingly, EGF mitigated some of the effects of Jagged1, by counteracting the raise in expression of *Jag2*, *Blbp* and *Prnp* (Fig. 7F, 7H, 7J). This suggests that EGFR activation partly opposes the action of the Notch pathway, notably in the control of the stemness marker BLBP.

We may thus conclude from these data that, EGFR, which is a target of the PrP^C-Notch signalling axis, exerts a negative feedback action on both PrP^C and Notch when it is activated. Thus, the induction of EGFR expression downstream from PrP^C appears to poise cells to respond to an EGF signal, which antagonizes stem cell maintenance and likely favours the conversion into a more mature neuronal progenitor state.

DISCUSSION

Although *Prnp*$^{-/-}$ mice develop without overt abnormalities [41], they have been instrumental in unveiling an unexpected involvement of PrP^{C} in the self-renewal of various stem/progenitor cells, most notably along the hematopoietic and neural lineages [5, 6]. Despite recent progress regarding the contribution of this protein to stem cell homeostasis [4], and notably to Hedgehog signalling [12], the cellular and molecular mechanisms at play are yet to be fully understood. Here, by combining *in vitro* and *in vivo* experiments, we uncover a critical role of PrP^{C} in the control of Notch signalling in neural progenitors, which in turn influences neural stem cell markers, N-cadherin-mediated cell contacts and EGFR expression. Our study further elaborates on an intricate interplay between Notch and EGFR signalling, as well as PrP^{C} expression itself.

Uncovering the PrP^{C}-Notch connection was facilitated by our *in vitro* models, the 1C11 neuronal progenitor and its PrP-KD derivatives [15], and primary neurospheres from WT and *Prnp*$^{-/-}$ mouse embryos. The defect in Notch signalling in PrP-depleted cells is evidenced by the prominent reduction in the expression of the Notch target gene *Hes1*. From a mechanistic point of view, our data reveal that the absence of PrP^{C} is associated with a dramatic decrease in the expression of the Notch ligands Jagged1 and Jagged2 as well as that of the Notch1/Notch3 receptors. From these cellular observations, screening early *Prnp*$^{-/-}$ embryos allowed us to delineate a narrow time-window when defects in the Notch pathway can be revealed under PrP^{C} ablation. Our analyses at various embryonic stages encompassing neural tube closure indicate that these defects initiate at E8.5-E9 and are most apparent at E9.5. This time-window corresponds to that of alterations in Hedgehog signalling and tubulin post-translational modifications that we recently uncovered in *Prnp*$^{-/-}$ embryos [12]. At these stages, PrP^{C} is abundantly expressed in the ventricular zone of the neural tube [12], where neural stem cells reside. As *in vitro* (PrP^{KD}-1C11 cells and neurospheres from *Prnp*$^{-/-}$

embryos), alterations monitored in the neural tubes of *Prnp*$^{-/-}$ embryos include reductions in the mRNA expression of both *Jag1* and *Jag2*, and their receptors *Notch1* and *Notch3*. The milder and temporally-restricted defects detected in neural tubes from *Prnp*$^{-/-}$ embryos, in contrast to our *in vitro* observations, might be accounted for by the co-existence of diverse cell types, whose relative number may vary depending on the developmental stage and the dorso-ventral and rostro-caudal axes. Another likely explanation would be the occurrence of dynamic mechanisms of adaptation *in vivo*, as recently described in the case of Hedgehog signalling [42]. Importantly, that the ablation of PrP^{C} compromises Notch signalling *in vivo* is firmly established by the strong reduction in the mRNA levels of the two Notch target genes *Hes5* and *Blbp*, starting from E8.5-E9. Because these genes specify neuroepithelial and radial glial cells in the developing CNS [21, 22], these data argue that the lack of PrP^{C} transiently affects the pool of early neural stem / progenitor cells and causes premature commitment. This conclusion is supported by the altered pattern of Ki67 in *Prnp*$^{-/-}$ embryos. The reduction in the expression of *Nestin* in neural tubes from *Prnp*$^{-/-}$ embryos at E9.5 and E10.5, together with an increase in *Olig2* expression at the latter stage, further corroborates this view. These changes at the mRNA level are accompanied by a partly disorganized pattern of Nestin staining at E9.5 and a subtle extension of the Olig2-positive domain at E10.5 in the absence of PrP^{C}. Overall, these data are in line with the positive regulation of Nestin expression by Notch [43] as well as with the recent demonstration that Notch activity influences dorso-ventral patterning of the neural tube by negatively regulating the expression of Olig2 [26].

A second contribution of this work is the demonstration that PrP^{C} depletion is associated with a disruption of N-cadherin-based cell-cell contacts. This alteration of cell architecture arises, at least partly, from defects in Notch signalling. Indeed, PrP^{KD}-1C11 cells exposed to Jagged1 restored N-cadherin-dependent intercellular contacts. These data fit in with the reported defects in apico-basal polarity of the neural tube in early embryos following blockade of the

Notch pathway [44] and with the notion that N-cadherin patterning is affected when apico-basal polarity is disrupted [45]. In line with our *in vitro* data and in agreement with the transient reduction in Notch signalling in the developing CNS of animals lacking PrP^C (see Fig. 2), we observed subtle defects in N-cadherin patterning in the neuroepithelium of *Prnp*$^{-/-}$ embryos. These alterations notably include shifted distribution from the apical face of the neuroepithelium towards the mantle zone. Because N-cadherin-mediated contacts participate to the maintenance of neuroepithelial progenitors in the ventricular zone [30], such defects further argue that PrP^C deficiency impacts on the proper expansion of the neural stem cell pool. In addition, in view of the link between cadherin-dependent contacts and β-catenin signalling [31], these data suggest that the lack of PrP^C affects the pool of β-catenin in neural stem and/or progenitor cells of the neuroepithelium, which may in turn impact on their proliferation / differentiation balance. Altogether, these findings add to the complex interplay between PrP^C and cadherins, since PrP^C was previously shown to contribute to the recruitment of E-cadherin at cell-cell contacts [46, 47] or to the trafficking of N-cadherin in differentiating neurons [48].

Our data finally posit EGFR as a third protagonist whose expression is affected by the absence of PrP^C. Reductions in EGFR expression were observed both *in vitro* in PrP^{KD}-1C11 cells and neurospheres from *Prnp*$^{-/-}$ embryos, as well as *in vivo* in *Prnp*$^{-/-}$ embryos. Thus, beyond impinging on EGFR activity as previously described [47, 49], PrP^C also contributes to the regulation of *Egfr* transcripts. In line with [36], we showed that EGFR expression is positively controlled by Notch signalling. Finally, upon EGF exposure, both Notch signalling and PrP^C (mRNA and protein) levels were toned down, suggesting that the induction of EGFR downstream from the PrP^C-Notch network poises cells to respond to an EGFR-activating stimulatory signal that will conversely dampen the PrP^C-Notch axis. In this respect, it is noteworthy that EGFR signalling contributes to the recruitment of neural progenitors

during development [34], or after injury [50]. According to our results, this process may involve a negative feedback on Notch and PrP^C.

Altogether, our study allows to propose a molecular cascade linking the various actors under the control of PrP^C (Figure S10): (1) PrP^C positively regulates the expression of Notch ligands and that of the Notch receptors and its ablation compromises Notch signalling; (2) proper Notch signalling supports N-cadherin-mediated cell-cell contacts and (3) exerts a positive feedback action on PrP^C; (4) downstream from PrP^C, Notch signalling additionally upregulates the expression of EGFR, which, when activated, (5) negatively regulates both PrP^C and Notch. Hence, our data strengthen the view that PrP^C, the Notch pathway and EGFR belong to a gene regulatory network, whose imbalance may shift towards "more stemness" (higher Notch activity induces higher PrP^C expression and vice-versa) or "less stemness" (EGFR activation dampens Notch signalling and PrP^C expression). In view of the established roles of these various actors in the self-renewal of neuroprogenitors [30, 37, 51], this global cascade ultimately supports the involvement of PrP^C in neural stem cell maintenance. *In vivo*, the changes observed in embryos lacking PrP^C may altogether favour a precocious differentiation of neural stem / progenitor cells (see above). The subtle and transient defects occurring in the developing CNS of *Prnp*$^{-/-}$ mice could actually account for the behavioural and cognitive deficits recorded in mice lacking PrP^C [52], in line with the proposed neurodevelopmental origin of psychiatric disorders [53]. Another hypothesis that would be worth considering is that the absence of PrP^C disturbs the homeostasis of adult neural stem cells, since Notch signalling controls neural stem cell maintenance in the adult brain as well [54]. Incidentally, the Notch pathway appears to be also affected by the lack of PrP^C after birth as the expression of *Jag2* mRNA fails to increase in the hippocampus of *Prnp*$^{-/-}$ mice during postnatal development, while *Jag1* mRNA level is higher in the same brain region of adult *Prnp*$^{-/-}$ mice versus their WT counterparts [55]. From a pathological point of view, the

latter observations added to our findings may have relevance as to the disturbed cell fate of adult neural stem cells upon prion infection [56].

CONCLUSION

In summary, our work demonstrates that PrP^C contributes to the regulation of a major developmental signalling pathway, namely Notch, and thereby supports the maintenance of neural stem cell architecture as well as EGFR expression. Beyond neural stem / progenitor cells, the molecular scenario brought to light in the present study may more broadly account for the contribution of PrP^C to the self-renewal of diverse types of stem cells within their niche. Since the overall protagonists shown here to be under the control of PrP^C sustain the self-renewal of HSCs in their bone marrow niche [57–59], our results may notably accommodate the requirement of PrP^C for the long-term maintenance of HSCs [5].

ACKNOWLEDGEMENTS

The authors thank Dr. C. Brou (Institut Pasteur, Paris) for the kind gift of Notch antibody, Céline Urien (INRA-Jouy) and the MIMA2 platform (INRA-Jouy) for access to confocal microscopy and Johan Castille for mouse breeding. This work was supported by funds from ARC (grant SFI2011205489) and INSERM to S.M.-R. S.M.-L. and T.Z.H. were supported by fellowships from DIM StemPole (Region Ile de France) and Fondation pour la Recherche Médicale, respectively. The J.-M.T laboratory was supported by grants from the Spanish Plan Nacional de I+D+I (RTA2012-00004 and AGL2012-37988-C04).

DISCLOSURE OF POTENTIAL CONFLICTS OF INTEREST

The authors indicate no potential conflicts of interest.

REFERENCES

1. Aguzzi A, Calella AM. Prions: protein aggregation and infectious diseases. Physiol Rev 2009;89(4):1105–52.
2. Linden R, Martins VR, Prado MA, et al. Physiology of the prion protein. Physiol Rev 2008;88(2):673–728.
3. Lopes MH, Santos TG. Prion potency in stem cells biology. Prion 2012;6(2):142–6.
4. Martin-Lanneree S, Hirsch TZ, Hernandez-Rapp J, et al. PrPC from stem cells to cancer. Front Cell Dev Biol 2014;2:55.
5. Zhang CC, Steele AD, Lindquist S, et al. Prion protein is expressed on long-term repopulating hematopoietic stem cells and is important for their self-renewal. Proc Natl Acad Sci U A 2006;103(7):2184–9.
6. Steele AD, Emsley JG, Ozdinler PH, et al. Prion protein (PrPc) positively regulates neural precursor proliferation during developmental and adult mammalian neurogenesis. Proc Natl Acad Sci U A 2006;103(9):3416–21.
7. Santos TG, Silva IR, Costa-Silva B, et al. Enhanced neural progenitor/stem cells self-renewal via the interaction of stress-inducible protein 1 with the prion protein. Stem Cells 2011;29(7):1126–36.
8. Liao MJ, Zhang CC, Zhou B, et al. Enrichment of a population of mammary gland cells that form mammospheres and have in vivo repopulating activity. Cancer Res 2007;67(17):8131–8.
9. Hidaka K, Shirai M, Lee JK, et al. The cellular prion protein identifies bipotential cardiomyogenic progenitors. Circ Res 2010;106(1):111–9.
10. Mouillet-Richard S, Laurendeau I, Vidaud M, et al. Prion protein and neuronal differentiation: quantitative analysis of prnp gene expression in a murine inducible neuroectodermal progenitor. Microbes Infect 1999;1(12):969–76.
11. Peralta OA, Huckle WR, Eyestone WH. Expression and knockdown of cellular prion protein (PrPC) in differentiating mouse embryonic stem cells. Differentiation 2011;81(1):68–77.
12. Halliez S, Martin-Lanneree S, Passet B, et al. Prion protein localizes at the ciliary base during neural and cardiovascular development and its depletion affects α-tubulin post-translational modifications. Sci Rep 2015;5:17146.
13. Mouillet-Richard S, Mutel V, Loric S, et al. Regulation by neurotransmitter receptors of serotonergic or catecholaminergic neuronal cell differentiation. J Biol Chem 2000;275(13):9186–92.
14. Mouillet-Richard S, Ermonval M, Chebassier C, et al. Signal transduction through prion protein. Science 2000;289(5486):1925–8.
15. Loubet D, Dakowski C, Pietri M, et al. Neuritogenesis: the prion protein controls beta1 integrin signaling activity. FASEB J 2012;26:678–690.
16. Herva ME, Relano-Gines A, Villa A, et al. Prion infection of differentiated neurospheres. J Neurosci Methods 2010;2010:3.
17. Fuccillo M, Joyner AL, Fishell G. Morphogen to mitogen: the multiple roles of hedgehog signalling in vertebrate neural development. Nat Rev Neurosci 2006;7(10):772–83.

18. Louvi A, Artavanis-Tsakonas S. Notch signalling in vertebrate neural development. Nat Rev Neurosci 2006;7(2):93–102.
19. Prusiner SB, Groth D, Serban A, et al. Ablation of the prion protein (PrP) gene in mice prevents scrapie and facilitates production of anti-PrP antibodies. Proc Natl Acad Sci U A 1993;90(22):10608–12.
20. Manson JC, Clarke AR, Hooper ML, et al. 129/Ola mice carrying a null mutation in PrP that abolishes mRNA production are developmentally normal. Mol Neurobiol 1994;8(2–3):121–7.
21. Basak O, Taylor V. Identification of self-replicating multipotent progenitors in the embryonic nervous system by high Notch activity and Hes5 expression. Eur J Neurosci 2007;25(4):1006–22.
22. Liu RZ, Mita R, Beaulieu M, et al. Fatty acid binding proteins in brain development and disease. Int J Dev Biol 2010;54(8–9):1229–39.
23. Tremblay P, Bouzamondo-Bernstein E, Heinrich C, et al. Developmental expression of PrP in the post-implantation embryo. Brain Res 2007;1139:60–7.
24. Del Amo FF, Smith DE, Swiatek PJ, et al. Expression pattern of Motch, a mouse homolog of Drosophila Notch, suggests an important role in early postimplantation mouse development. Development 1992;115(3):737–44.
25. Copp AJ, Greene ND, Murdoch JN. The genetic basis of mammalian neurulation. Nat Rev Genet 2003;4(10):784–93.
26. Kong JH, Yang L, Dessaud E, et al. Notch activity modulates the responsiveness of neural progenitors to sonic hedgehog signaling. Dev Cell 2015;33(4):373–87.
27. Guichet PO, Guelfi S, Teigell M, et al. Notch1 stimulation induces a vascularization switch with pericyte-like cell differentiation of glioblastoma stem cells. Stem Cells 2015;33(1):21–34.
28. Rowitch DH. Glial specification in the vertebrate neural tube. Nat Rev Neurosci 2004;5(5):409–19.
29. Farkas LM, Huttner WB. The cell biology of neural stem and progenitor cells and its significance for their proliferation versus differentiation during mammalian brain development. Curr Opin Cell Biol 2008;20(6):707–15.
30. Rousso DL, Pearson CA, Gaber ZB, et al. Foxp-mediated suppression of N-cadherin regulates neuroepithelial character and progenitor maintenance in the CNS. Neuron 2012;74(2):314–30.
31. Miyamoto Y, Sakane F, Hashimoto K. N-cadherin-based adherens junction regulates the maintenance, proliferation, and differentiation of neural progenitor cells during development. Cell Adh Migr 2015;9(3):183–92.
32. Chen X, Stoeck A, Lee SJ, et al. Jagged1 expression regulated by Notch3 and Wnt/beta-catenin signaling pathways in ovarian cancer. Oncotarget 2010;1(3):210–8.
33. Hamidi H, Gustafason D, Pellegrini M, et al. Identification of novel targets of CSL-dependent Notch signaling in hematopoiesis. Plos One 2011;6(5):e20022.
34. Burrows RC, Wancio D, Levitt P, et al. Response diversity and the timing of progenitor cell maturation are regulated by developmental changes in EGFR expression in the cortex. Neuron 1997;19(2):251–67.
35. Caric D, Raphael H, Viti J, et al. EGFRs mediate chemotactic migration in the developing telencephalon. Development 2001;128(21):4203–16.

36. Andreu-Agullo C, Morante-Redolat JM, Delgado AC, et al. Vascular niche factor PEDF modulates Notch-dependent stemness in the adult subependymal zone. Nat Neurosci 2009;12(12):1514–23.
37. Aguirre A, Rubio ME, Gallo V. Notch and EGFR pathway interaction regulates neural stem cell number and self-renewal. Nature 2010;467(7313):323–7.
38. Ottone C, Krusche B, Whitby A, et al. Direct cell-cell contact with the vascular niche maintains quiescent neural stem cells. Nat Cell Biol 2014;16(11):1045–56.
39. Yoo AS, Bais C, Greenwald I. Crosstalk between the EGFR and LIN-12/Notch pathways in C. elegans vulval development. Science 2004;303(5658):663–6.
40. Hasson P, Egoz N, Winkler C, et al. EGFR signaling attenuates Groucho-dependent repression to antagonize Notch transcriptional output. Nat Genet 2005;37(1):101–5.
41. Halliez S, Passet B, Martin-Lanneree S, et al. To develop with or without the prion protein. Front Cell Dev Biol 2014;2:58.
42. Cohen M, Kicheva A, Ribeiro A, et al. Ptch1 and Gli regulate Shh signalling dynamics via multiple mechanisms. Nat Commun 2015;6:6709.
43. Shih AH, Holland EC. Notch signaling enhances nestin expression in gliomas. Neoplasia 2006;8(12):1072–82.
44. Main H, Radenkovic J, Jin SB, et al. Notch signaling maintains neural rosette polarity. Plos One 2013;8(5):e62959.
45. Higginbotham H, Guo J, Yokota Y, et al. Arl13b-regulated cilia activities are essential for polarized radial glial scaffold formation. Nat Neurosci 2013;16(8):1000–7.
46. Solis GP, Radon Y, Sempou E, et al. Conserved roles of the prion protein domains on subcellular localization and cell-cell adhesion. Plos One 2013;8(7):e70327.
47. Solis GP, Schrock Y, Hulsbusch N, et al. Reggies/flotillins regulate E-cadherin-mediated cell contact formation by affecting EGFR trafficking. Mol Biol Cell 2012;23(10):1812–25.
48. Bodrikov V, Solis GP, Stuermer CA. Prion protein promotes growth cone development through reggie/flotillin-dependent N-cadherin trafficking. J Neurosci 2011;31(49):18013–25.
49. Llorens F, Carulla P, Villa A, et al. PrP(C) regulates epidermal growth factor receptor function and cell shape dynamics in Neuro2a cells. J Neurochem 2013;127(1):124–38.
50. Aguirre A, Dupree JL, Mangin JM, et al. A functional role for EGFR signaling in myelination and remyelination. Nat Neurosci 2007;10(8):990–1002.
51. Codega P, Silva-Vargas V, Paul A, et al. Prospective identification and purification of quiescent adult neural stem cells from their in vivo niche. Neuron 2014;82(3):545–59.
52. Schmitz M, Greis C, Ottis P, et al. Loss of Prion Protein Leads to Age-Dependent Behavioral Abnormalities and Changes in Cytoskeletal Protein Expression. Mol Neurobiol 2014.
53. Markham JA, Koenig JI. Prenatal stress: role in psychotic and depressive diseases. Psychopharmacol. Berl 2010;214(1):89–106.
54. Pierfelice T, Alberi L, Gaiano N. Notch in the vertebrate nervous system: an old dog with new tricks. Neuron 2011;69(5):840–55.

55. Benvegnu S, Roncaglia P, Agostini F, et al. Developmental influence of the cellular prion protein on the gene expression profile in mouse hippocampus. Physiol Genomics 2011;43(12):711–25.
56. Relano-Gines A, Gabelle A, Hamela C, et al. Prion replication occurs in endogenous adult neural stem cells and alters their neuronal fate: involvement of endogenous neural stem cells in prion diseases. Plos Pathog 2013;9(8):e1003485.
57. Doan PL, Himburg HA, Helms K, et al. Epidermal growth factor regulates hematopoietic regeneration after radiation injury. Nat Med 2013;19(3):295–304.
58. Hosokawa K, Arai F, Yoshihara H, et al. Cadherin-based adhesion is a potential target for niche manipulation to protect hematopoietic stem cells in adult bone marrow. Cell Stem Cell 2010;6(3):194–8.
59. Poulos MG, Guo P, Kofler NM, et al. Endothelial Jagged-1 is necessary for homeostatic and regenerative hematopoiesis. Cell Rep 2013;4(5):1022–34.

FIGURE LEGENDS

Figure 1: PrP^{C} depletion compromises Notch signalling in neural stem /progenitor cells.

(A) The Notch target gene *Hes1* is downregulated in PrP^{KD}-1C11 cells as measured in qRT-PCR. Further qRT-PCR analysis of effectors of the Notch pathway in 1C11 cells and their PrP-KD derivatives indicates that PrP^{C} silencing drastically reduces Jagged1 (*Jag1*) and Jagged2 (*Jag2*) expression (B). *Notch1* level is strongly decreased and *Notch2* slightly reduced in PrP-depleted 1C11 cells while *Notch3* level is upregulated (C). Neurospheres from *Prnp*$^{-/-}$ embryos exhibit reduced *Hes1* (D), *Jag1*, *Jag2* (E) as well as *Notch1* and *Notch3* (F) mRNAs as compared with WT controls. The protein levels of Jagged1 (G, I) and Notch1 (H, J) measured through western blot and normalized to α-tubulin (α-tub) (G, H) or actin (I, J) are drastically reduced in PrP^{KD}-1C11 cells and *Prnp*$^{-/-}$ NSC versus their PrP^{C}-expressing counterparts. Data are representative of a set of n=3 independent experiments. Results are expressed as means ± s.e.m. * $p<0.05$, ** $p<0.01$ versus control (Student's *t*-test).

Figure 2: The Notch pathway is affected in neural tubes from embryos lacking PrP^{C}, together with the expression of NSC and cell fate specification markers.

Quantitative PCR analysis of the expression of *Jag1*, *Jag2* (A, F), *Notch1*, *Notch2*, *Notch3* (B, G), the Notch target genes *Hes5* and *Blbp* (C, H), the neural stem cell markers *Sox2*, *Nestin* and *Pax6* (D, I), the motor neuron progenitor marker *Olig2* and the oligodendrocyte progenitor marker *PDGFRα* (E, J) was performed in neural tube-enriched samples from *Prnp*$^{-/-}$ early embryos and WT controls at E9.5 and E10.5. In neural tubes from E9.5 *Prnp*$^{-/-}$ embryos (n=5), reduced mRNA levels are observed for *Jag1* and *Jag2* (A), *Notch1* and *Notch3* (B), *Hes5* and *Blbp* (C) as compared with neural tubes from WT controls. These changes are accompanied by reduced levels of *Sox2* and *Nestin* (D). In neural tubes from E10.5 *Prnp*$^{-/-}$ embryos (n=6), *Jag1* (F) and *Notch1* (G) levels are slightly increased while *Blbp* (H) and *Nestin* (I) level remains lower than in neural tubes from WT embryos. At this stage, *Olig2* transcripts are significantly increased in *Prnp*-ablated neural tubes (J). Results are expressed as means ± s.e.m. * $p<0.05$, ** $p<0.01$ versus control (Student's *t*-test).

Figure 3: *Prnp*$^{-/-}$ embryos exhibit altered Nestin distribution, as well as Ki67 and Olig2 staining *in vivo*

(A) Transverse sections of the neuroepithelium at the level of the presumptive hindbrain (top) or mid-trunk region (bottom) from WT (left) and *Prnp*$^{-/-}$ (right) mouse embryos at E9.5 co-stained for Nestin (green) and DAPI (blue) (scale bar 20 μm). (B) Transverse sections of the neuroepithelium at the level of the trunk region from WT (left) and *Prnp*$^{-/-}$ (right) mouse embryos at E10.5 co-stained for Ki67 (red) and nuclear marker DAPI (blue) (scale bar: 20 μm). (C) Transverse sections of the neuroepithelium at the level of the trunk region from WT (left) and *Prnp*$^{-/-}$ (right) mouse embryos at E10.5 co-stained for Olig2 (red) and DAPI (blue) (scale bar: 20 μm). Images are representative of a set of n=3 to 6 *Prnp*$^{-/-}$ embryos and n=3 to 6 WT embryos.

Figure 4: PrP^{C} depletion affects N-cadherin distribution *in vitro* and *in vivo*

(A) PrP^{C}-deficient 1C11 cells exhibit drastic changes in N-cadherin and β-catenin staining associated with disrupted cell-cell contacts, as compared to 1C11 cells. Scale bar = 20 μm. (B) Western blot analysis of PrP^{KD}-1C11 cell extracts indicates increased N-cadherin and decreased β-catenin protein expression. Protein levels were normalized to α-tubulin (α-tub). Data are representative of n=3 independent experiments. (C) Transverse section of the neuroepithelium at the level of the presumptive caudal trunk region from WT (left) and *Prnp*$^{-/-}$ (right) mouse embryos at E9.5 co-stained for N-cadherin (green) and DAPI (blue) (scale bar: 10 μm). (D-E) Relative distribution of N-cadherin staining intensity from the lumen to the pial surface of the neural tube in WT (D) and *Prnp*$^{-/-}$ (E) embryos. Images are representative of n=3 embryos of each genotype.

Figure 5: Restoring an active Notch pathway in PrP^{KD}-1C11 cells induces N-cadherin dependent cell contacts

(A-C) PrP^{KD}-1C11 cells were grown on Jagged1-coated dishes and mRNAs encoding the Notch ligands *Jag1* and *Jag2* (A), receptors *Notch1*, *Notch2*, *Notch3* (B) and target gene *Hes1* (C) were measured through qRT-PCR. (D) qRT-PCR analysis of *N-cad* expression in PrP^{KD}-1C11 cells grown on Jagged1-coated dishes shows similar level as in control PrP^{KD}-1C11 cells. (E) Western blot analysis of N-cadherin expression in PrP^{KD}-1C11 cells grown on Jagged1-coated dishes reveals higher level as compared with control PrP^{KD}-1C11 cells. Protein levels were normalized to α-tubulin (α-tub). (F) PrP^{KD}-1C11 cells grown on Jagged1-coated dishes were stained with antibodies against N-cadherin or β-catenin . Scale bar = 20

μm. Results in (A-D) are expressed as means ± s.e.m. of n=3 independent experiments. * $p<0.05$, ** $p<0.01$ versus control (Student's *t*-test).

Figure 6: PrP^{C} positively controls EGFR expression via the Notch pathway

(A-D) Quantitative PCR and western blot analyses indicate that EGFR mRNA (A, C) and protein (B, D) levels are reduced in PrP^{KD}-1C11 cells versus their parental 1C11 cells (A, B) as well as in *Prnp*$^{-/-}$ versus WT NSC (C, D). (E) Quantitative PCR analysis of *Egfr* expression performed in neural tube-enriched samples from *Prnp*$^{-/-}$ early embryos and WT controls at E9, E9.5 and E10.5 reveals reduced levels at all stages in the absence of PrP^{C} (n=3 to 6 samples each). (F-G) Quantitative PCR and western blot analyses indicate that EGFR mRNA (F) and protein (G) levels are enhanced in PrP^{KD}-1C11 cells grown on Jagged1-coated dishes as compared to untreated PrP^{KD}-1C11 cells. Protein levels were normalized to α-tubulin (α-tub) (B, G) or actin (D). Data shown on (A-D) and (F-G) are representative of a set of n=3 independent experiments. Results are expressed as means ± s.e.m. * $p<0.05$, ** $p<0.01$ versus control (Student's *t*-test).

Figure 7: EGFR exerts a negative feedback action on Notch signalling and PrP^{C} expression

(A-D) 1C11 cells were exposed to EGF (10ng/ml, 24h) and mRNAs encoding the Notch ligands *Jag1* and *Jag2* (A), receptors *Notch1*, *Notch2*, *Notch3* (B) and target gene *Hes1* and *Blbp* (C), as well as *Prnp* (D) were measured through qRT-PCR. (E) Western blot analysis of PrP^{C} expression in cell extracts from 1C11 cells exposed or not to EGF (10ng/ml, 24h). Middle panel shows full-length PrP^{C} deglycosylated with PNGaseF-treatment. Protein levels were normalized to α-tubulin (α-tub). Data shown are representative of a set of n=3 independent experiments. (F-J) 1C11 cells were grown on Jagged1-coated dishes and

concomitantly exposed or not to EGF (10ng/ml, 24h). *Jag1*, *Jag2* (F), *Notch1*, *Notch2*, *Notch3* (G) *Hes1*, *Blbp* (H), *Egfr* (I) and *Prnp* (J) mRNAs were measured through qRT-PCR. Results are expressed as means ± s.e.m. of n=4 independent experiments. * $p<0.05$, ** $p<0.01$ versus control (Student's *t*-test).

Supplemental Figure 1: Altered Notch nuclear staining in PrP^{C}-depleted 1C11 cells. 1C11 cells but not their PrP-null derivatives exhibit nuclear Notch staining, indicating that Notch pathway is active in 1C11 cells and switched off in PrP-depleted cells. Scale bar = 20 µm.

Supplemental Figure 2: The Notch pathway is affected in early embryos lacking PrP^{C}.

Quantitative PCR analysis of *Jag1*, *Jag2* (A, D), *Notch1*, *Notch2*, *Notch3* (B, E) and the Notch target genes *Hes5* and *Blbp* (C, F) expression was performed in $Prnp^{-/-}$ early embryos and WT controls at E8.5 (A-C) or neural tubes from $Prnp^{-/-}$ embryos and WT controls at E9 (D-F). At E8.5 $Prnp^{-/-}$ whole embryos exhibited reduced *Jag2* (A), as well as *Blbp* mRNAs (C) as compared with WT controls. To the opposite, mild increases in *Notch1* and *Notch2* levels were monitored (B). In neural tubes from E9 $Prnp^{-/-}$ embryos, reduced mRNA levels are observed for *Jag2* (D), *Notch1* (E), *Hes5* and *Blbp* (F) as compared with neural tubes from WT controls. Results are expressed as means ± s.e.m and are representative of a set of n=3 independent experiments. * $p<0.05$, ** $p<0.01$ versus control (Student's *t*-test).

Supplemental Figure 3: Expression pattern of Nestin in *Prnp-/-* and WT embryos at embryonic day E10.5.

Transverse sections of the neuroepithelium at the level of the trunk region from WT (top) and $Prnp^{-/-}$ (bottom) mouse embryos at E10.5 co-stained for Nestin (green) and nuclear marker

DAPI (blue) (scale bar: 30 μm). Images are representative of a set of n=3 *Prnp*$^{-/-}$ embryos and n=3 WT embryos.

Supplemental Figure 4: Expression pattern of Ki67 in *Prnp-/-* and WT embryos at embryonic day E9.5.

Transverse section of the neuroepithelium at the level of the presumptive hindbrain (top) or mid-trunk region (bottom) from WT (left) and *Prnp*$^{-/-}$ (right) co-stained for Ki67 (red) and DAPI (blue). (scale bars: 50 and 20 μm for top and bottom panels, respectively). Images are representative of n=3 embryos analysed.

Supplemental Figure 5: Impact of transient PrP^{C} depletion in 1C11 cells on N-cadherin and F-actin staining.

1C11 cells transfected for 48h with a scramble siRNA used as control or two distinct siRNA targeting PrP^{C} (siPrP1, siPrP2) were stained with antibodies against N-cadherin (green) or phalloidin (red) to monitor F-actin. Alterations monitored after transient PrP^{C} silencing recapitulate those observed in stably PrP^{C}-depleted 1C11 cells (PrP^{KD}-1C11). Scale bar 20 μM.

Supplemental Figure 6: Impact of transient PrP^{C} depletion in 1C11 cells on β-catenin staining.

1C11 cells transfected for 48h with a scramble siRNA used as control or two distinct siRNA targeting PrP^{C} (siPrP1, siPrP2) were stained with antibodies against β-catenin (green).

Alterations monitored after transient PrP^{C} silencing recapitulate those observed in stably PrP^{C}-depleted 1C11 cells (PrP^{KD}-1C11). Scale bar 20 μM.

Supplemental Figure 7: Efficiency of transient PrP^{C} depletion in 1C11 cells.

1C11 cells transfected for 48h with a scramble siRNA used as control (left panel) or two distinct siRNA targeting PrP^{C} (siPrP1, middle panel, siPrP2, right panel) were stained with antibodies against PrP^{C} to check the efficiency of PrP^{C} silencing. Scale bar 20 μM.

Supplemental Figure 8: N-cadherin and β-catenin expression in PrP^{KD}-1C11 cells and N-cadherin expression in neural tubes from embryos lacking PrP^{C}.

(A) qRT-PCR analyses reveal increased N-cadherin (*N-cad*) expression in PrP-depleted 1C11 cells, and unchanged expression of β-catenin (*ß-cat*). (B) Quantitative PCR analysis of *N-cad* performed in neural tube-enriched samples of *Prnp*$^{-/-}$ embryos and WT controls at E9, E9.5 and E10.5, showing unaffected *N-cad* expression in the absence of PrP^{C} (n=3 to 6 independent experiments). ** $p<0.01$ versus control (Student's *t*-test).

Supplemental Figure 9: Expression pattern of N-cadherin in the mouse embryo at embryonic day E8.5.

Transverse sections of the neuroepithelium at the level of the presumptive from WT (left) and *Prnp*$^{-/-}$ (right) mouse embryos at E8.5 co-stained for N-cadherin (red) and DAPI (blue) (top panels, scale bar: 25 μm). Bottom panels are single optical sections from confocal microscopy imaging of sections stained for N-cadherin (scale bar: 10 μm). N-cadherin staining is

observed in the neuroepithelium, the notochord (nt) and in the somites (som) with a more diffuse signal in neuroepithelium portions of *Prnp*$^{-/-}$ vs. WT embryos. Confocal imaging of N-cadherin staining in the neuroepithelium of *Prnp*$^{-/-}$ embryos reveals zones with a wider, more diffused staining pattern across the thickness of the neural tube. Images are representative of n=4 embryos of each genotype.

Supplemental Figure 10: Summary scheme

(1) PrP^{C} positively regulates the expression of Notch ligands and that of the Notch receptors and its ablation compromises Notch signalling ; (2) proper Notch signalling supports N-cadherin-mediated cell-cell contacts and (3) exerts a positive feedback action on PrP^{C} ; (4) downstream from PrP^{C}, Notch signalling additionally upregulates the expression of EGFR, which, when activated, (5) negatively regulates both PrP^{C} and Notch. Thus, PrP^{C}, the Notch pathway and EGFR belong to a gene regulatory network, whose imbalance may shift towards "more stemness" (higher Notch activity induces higher PrP^{C} expression and vice-versa) or "less stemness" (EGFR activation dampens Notch signalling and PrP^{C} expression).

Legend to graphical abstract

Model for PrP^{C} action on Notch and stemness in neural progenitors:

- PrP^{C} positively regulates the expression of Notch ligands and that of the Notch receptors and its ablation compromises Notch signalling ;
- proper Notch signalling supports N-cadherin-mediated cell-cell contacts as well as the expression of NSC markers and exerts a positive feedback action on PrP^{C} ;

- downstream from PrP^C, Notch signalling additionally upregulates the expression of EGFR, which, when activated, negatively regulates both PrP^C and Notch.

Thus, PrP^C, the Notch pathway and EGFR belong to a gene regulatory network, whose imbalance may shift towards "more stemness" (higher Notch activity induces higher PrP^C expression and vice-versa) or "less stemness" (EGFR activation dampens Notch signalling and PrP^C expression).

Supplemental Materials and Methods

Reagents

All tissue culture reagents were from Invitrogen (Carlsbad, CA, USA). 4',6-diamidino-2-phenylindole (DAPI), TRITC-phalloidin and mouse monoclonal antibody against α-tubulin were from Sigma-Aldrich (St. Louis, MO, USA). Recombinant rat Jagged1-Fc, IgG1-Fc and EGF were from R&D systems (Minneapolis, MN, USA). Polyclonal rabbit antibodies against Jagged1, Notch1 and EGFR were from Cell Signalling Technology (Danvers, MA, USA). Mouse monoclonal antibodies against PrP^C (SAF32, Sha31) were from SPI-Bio (Montigny Le Bretonneux, France). Rabbit polyclonal antibody to Notch was a kind gift of C. Brou, Institut Pasteur, Paris, France. Monoclonal mouse antibodies against N-cadherin β–catenin, and Nestin were from BD Biosciences (Franklin Lakes, NJ, USA). Rabbit polyclonal antibody to Ki67 was from Abcam (Cambridge, UK). Mouse monoclonal antibodies against actin and Olig2 were from Novus Biologicals (Littleton, CO, USA) and Millipore (Temecula, CA, USA), respectively. PNGaseF was from New England Biolabs (Ipswich, MA, USA).

Immunofluorescence on Cells

Cells grown on labtek chambers (Nunc, Rochester, NY, USA) were washed in PBS and fixed with 4% formaldehyde in PBS. Cells were then permeabilized with blocking buffer (PBS with 20mM Glycine, 1% goat serum and 0.1% Triton X-100) for 15 minutes at room temperature. Cells were next incubated with primary antibody (5 μg/mL) diluted in PBS enriched with 1% goat serum and 0.1% Tween for 1 hour at room temperature. Cells were then incubated with Alexa Fluor 488 secondary antibodies (4 μg/mL) (Molecular Probes, Eugene, OR, USA) and DAPI, used as nuclear marker. Immunolabelling was observed and images recorded using a Zeiss

LSM 510 confocal microscope (Carl Zeiss Meditec France SAS, Le Pecq, France) using a Zeiss 63x Plan-Apochromat O.N. = 1,4 / Oil / DIC objective and LSM Image Browser.

Immunofluorescence on Embryos

Embryos were fixed with 4% paraformaldehyde overnight (ON) at 4°C, cryoprotected with sucrose, included in Freeze gel (Labonord) then frozen on dry ice and cryosectioned (14 μm) on a cryostat (Leica CM-3050-S). Sections were incubated ON at 4°C with the distinct primary antibodies followed by appropriate Alexa Fluor-conjugated secondary antibodies (Molecular Probes). Nuclei were stained using DAPI. Sections were finally mounted in Fluoromount (Sigma) and imaged on a Zeiss Axio Observer.Z1 microscope equipped with a CoolSNAP HQ2 camera (Photometrics). Z-series were acquired on a Zeiss LSM 700 confocal microscope. Images were analyzed with ImageJ and when necessary with the Bio-Formats plugin. Quantification of the Olig2-positive zone was performed by measuring its relative height versus that of the neural tube. WT and *Prnp*$^{-/-}$ embryos were compared paired-wise to ensure comparison within an identical section along the rostro-caudal axis.

Transient siRNA-mediated PrP^{C} silencing

1C11 cells were transfected for 48h with siRNA sequences (30 nM) using the Lipofectamine 2000 reagent according to the manufacturer's instructions (Invitrogen). Specific siRNA sequences used were: 5'-CAGUACAGCAACCAGAACATT-3' (sense siPrP1), 5'-UCGUGCACGACUGCGUCAAUATT-3' (sense siPrP2) and 5'-AACGAUGACACGAACACACTT-3' (sense scramble).

Preparation of protein extracts and western blot analyses

Cells were washed in PBS and incubated for 30 minutes at 4°C in NaDOC lysis buffer [50 mM Tris·HCl (pH 7.4)/150 mM NaCl/5 mM EDTA/0.5% Triton X-100/0.5% sodium deoxycholate] and a mixture of phosphatase (Thermo-Scientific, Waltham, MA, USA) and protease (Roche, Mannheim, Germany) inhibitors. Extracts were centrifuged at 14,000 x *g* for 15 minutes. Protein concentrations in the supernatant were measured by using the bicinchoninic acid method (Pierce, Rockford, IL, USA). Deglycosylation was performed on 15 µg of proteins with 500U PNGaseF for 1h at 37°C. Protein extracts (15 µg) were resolved by 4-12% SDS-PAGE (Invitrogen) and transferred to nitrocellulose membranes (iBlot, Invitrogen). Membranes were blocked with SEABLOCK blocking buffer (Thermo-Scientific) for 1 hour at room temperature and then incubated overnight at 4°C with primary antibody. Bound antibody was revealed by infrared detection using a secondary antibody coupled to IRDye fluorophores (Li-Cor biosciences, Lincoln, NE, USA). Western blot read out was performed with the Odyssey Infrared Imaging System (Li-Cor biosciences).

Isolation of total RNA and reverse transcriptase-polymerase chain reaction analysis

RNA was isolated by using the RNeasy extraction kit (Qiagen, Limburg, Netherlands) as recommended by the manufacturer's instructions. For reverse transcriptase-polymerase chain reaction (RT-PCR) analysis, first-strand cDNA was synthesized with oligo(dT) primer and random 6mers, using the PrimeScript reverse transcriptase kit (Takara, Shiga, Japan) according to the manufacturer's protocol. Real-time PCR was performed using Absolute QPCR SYBR Green ROX Mix (Thermo-Scientific, Waltham, MA, USA) on a ABI PRISM 7900HT (Applied biosystems, Life Technologies Corporation, Carlsbad, CA, USA). Real-time PCR analyzes was performed with the SDS software 2.3 (Applied biosystems). Primers used for the PCR reactions

are shown on Supplemental Table 1.

Supplemental Table 1: list of primers used for qRT-PCR experiments

mRNA	qPCR primer	
Tbp	forward	5'-CAAACCCAGAATTGTTCTCCTT -3'
	reverse	5'-ATGTGGTCTTCCTGAATCCCT-3'
Jag1	forward	5'- GGGAACCCTGTCAAGGAAAT-3'
	reverse	5'- GAGCTCAGCAGAGGAACCAG-3'
Jag2	forward	5'-GGCAAAGAATGCAAAGAAGC-3'
	reverse	5'-GCTCAGCATTGATGCAGGTA-3'
Notch1	forward	5'-ATGTCAATGTTCGAGGACCAG-3'
	reverse	5'-TCACTGTTGCCTGTCTCAAG-3'
Notch2	forward	5'-GTGGCAGAGTTGATCAATTG-3'
	reverse	5'-ATATCTCTGTTGGCCCCATTC-3'
Notch3	forward	5'-GGGTCCTGAGGTGATCGGCT-3'
	reverse	5'-AGGGTGCTGTGTTCTCGC-3'
Notch4	forward	5'- ATCACAGGATGACTGGCCTC-3'
	reverse	5'- ACTCGTACGTGTCGCTTCCT-3'
Hes1	forward	5'-CTACCCCAGCCAGTGTCAAC-3'
	reverse	5'-ATGCCGGGAGCTATCTTTCT-3'
Hes5	forward	5'-GGGGTTGTTTTGTGTTTGCA-3'
	reverse	5'-GGCCCTGAAGAAAGTCCTCT-3'
Blbp	forward	5'-GGAAGCTGACAGACAGTCAGA-3'
	reverse	5'-CGCCCAGAGCTTTCATGTAC-3'
N-cadh	forward	5'-CAAGAGCTTGTCAGAATCAGG-3'
	reverse	5'-CATTTGGATCATCCGCATC-3'
β-cat	forward	5'-GAGCTGCCATGTTCCCTGAGA-3'
	reverse	5'-CAAGTTCCGCGTCATCCTGATA-3'
Egfr	forward	5'-TGAGCAACATGTCAATGGACTTAC-3'
	reverse	5'-TTTGGTCAATTTCTGGCAGTTCTC-3'
Prnp	forward	5'-TTGGCAACGACTGGGAGGAC-3'
	reverse	5'-GGACTCCTTCTGGTACTGGGTGA-3'
Sox2	forward	5'-GCGGAGTGGAAACTTTTGTCC-3'
	reverse	5'-CGGGAAGCGTGTACTTATCCTT-3'
Pax6	forward	5'-GCCCTTCCATCTTTGCTTGGGAAA-3'
	reverse	5'-TAGCCAGGTTGCGAAGAACTCTGT-3'

Nestin	forward	5'-AGGAGAAGCAGGGTCTACAGAG -3'
	reverse	5'-GGTCAGGAAAGCCAAGAGAAG-3'
Olig2	forward	5'-TATTACAGACCGAGCCAACACC-3'
	reverse	5'-GGGCAGAAAAAGATCATCGGG-3'
PDGFRα	forward	5'-CAAACCCTGAGACCACAATG-3'
	reverse	5'-TCCCCCAACAGTAACCCAAG-3'

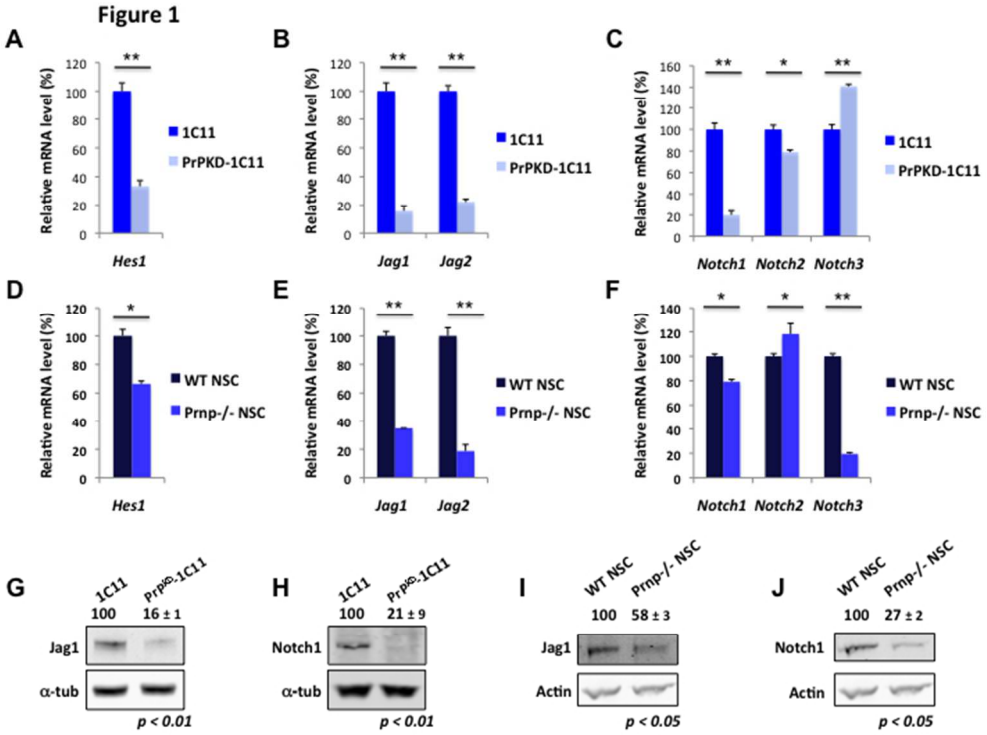

Figure 1

254x190mm (72 x 72 DPI)

Figure 2

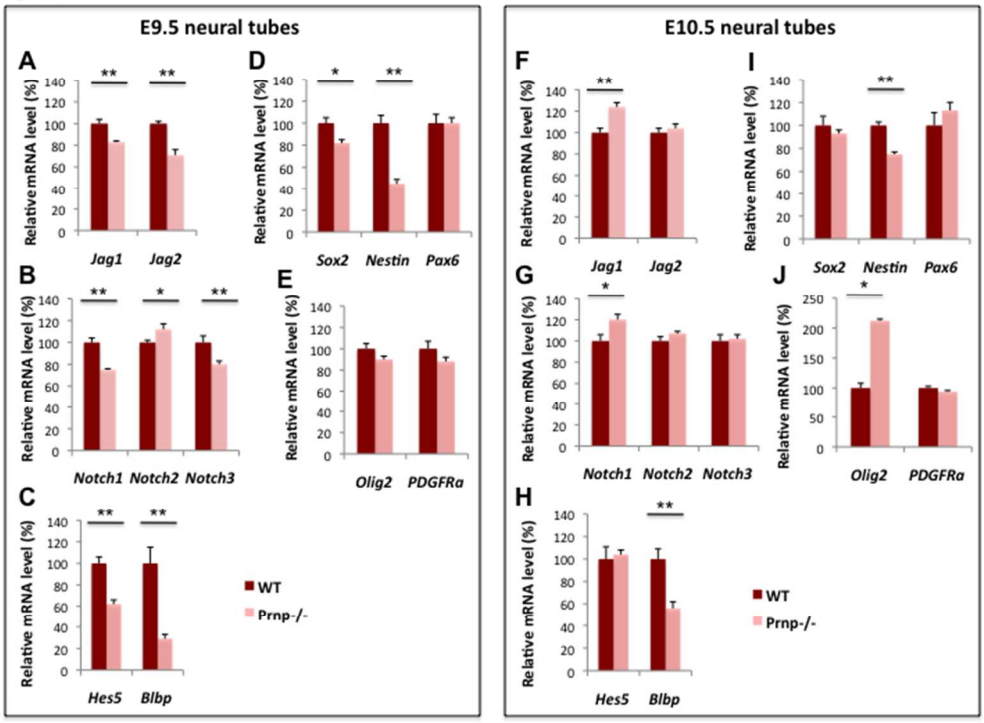

Figure 2

254x190mm (72 x 72 DPI)

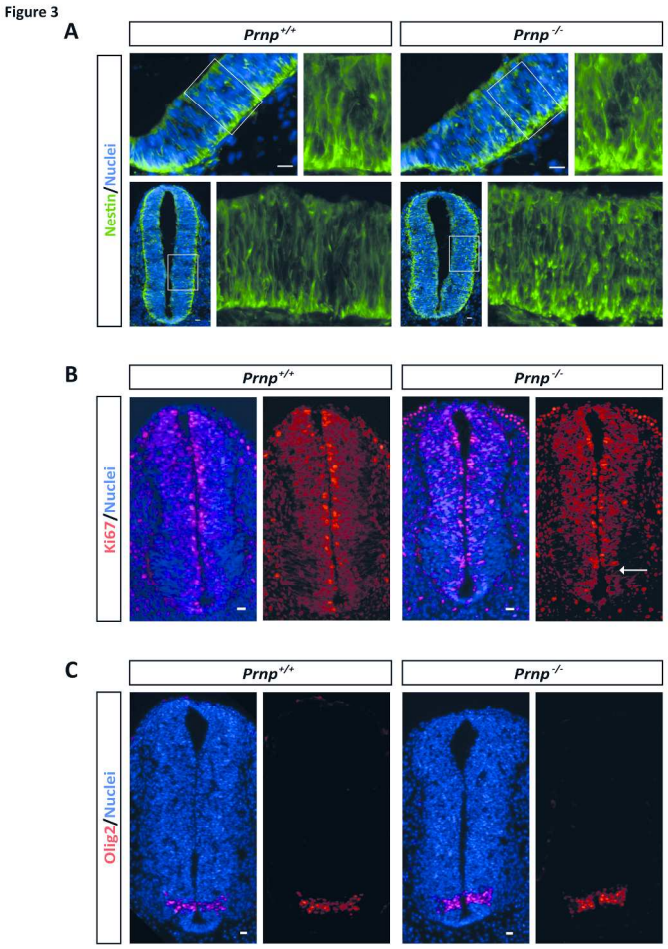

Figure 3

215x308mm (300 x 300 DPI)

Figure 4

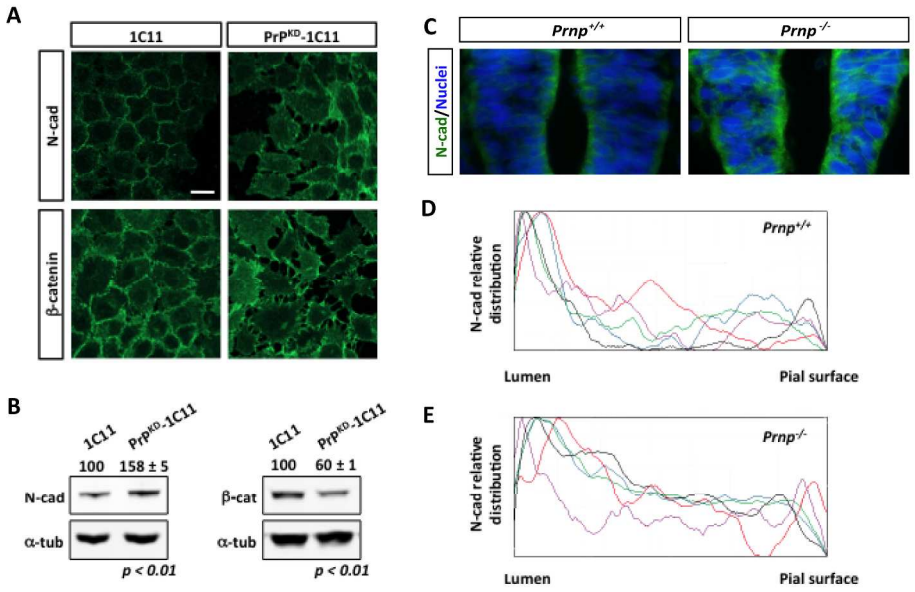

Figure 4

254x190mm (300 x 300 DPI)

Figure 5

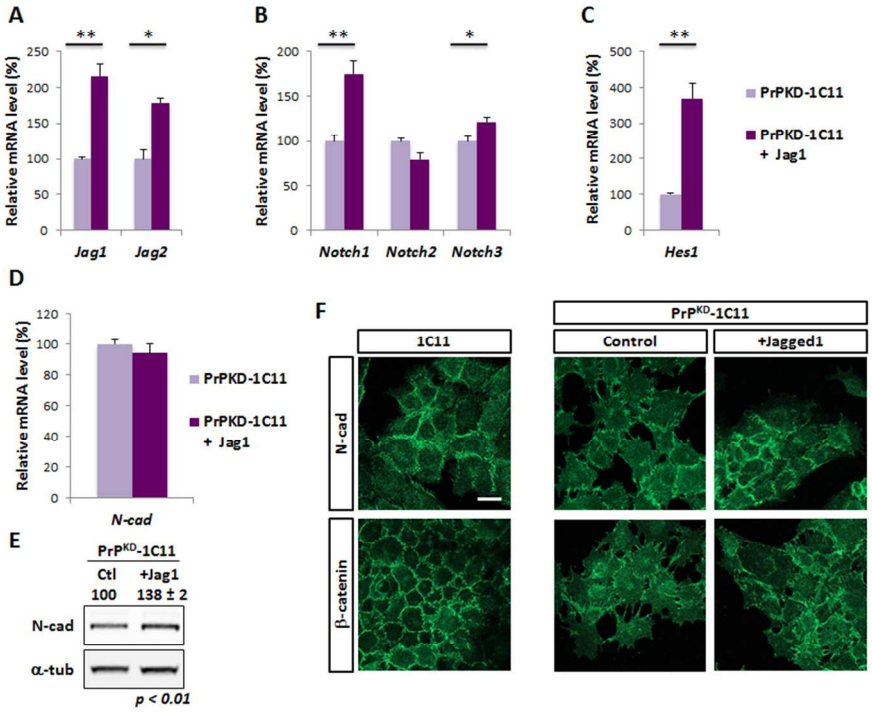

Figure 5

80x65mm (300 x 300 DPI)

Figure 6

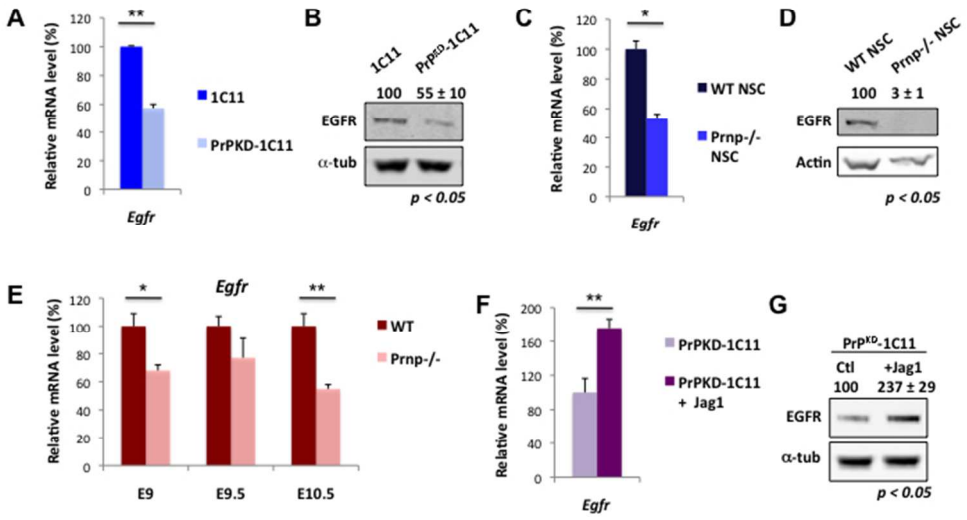

Figure 6

254x190mm (72 x 72 DPI)

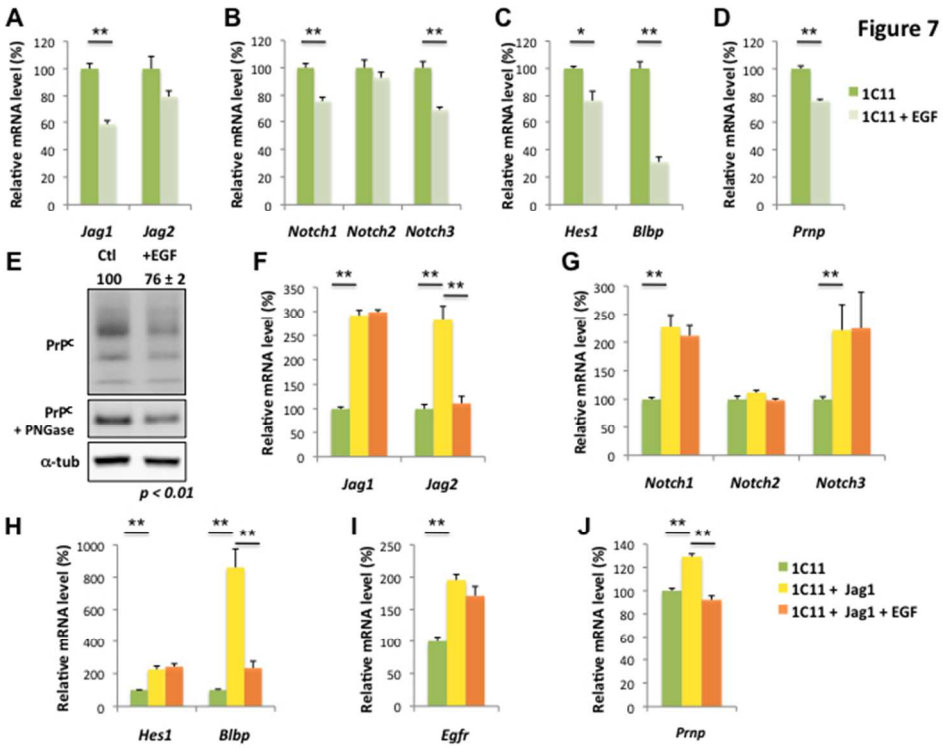

Figure 7

254x190mm (72 x 72 DPI)

S1 Fig

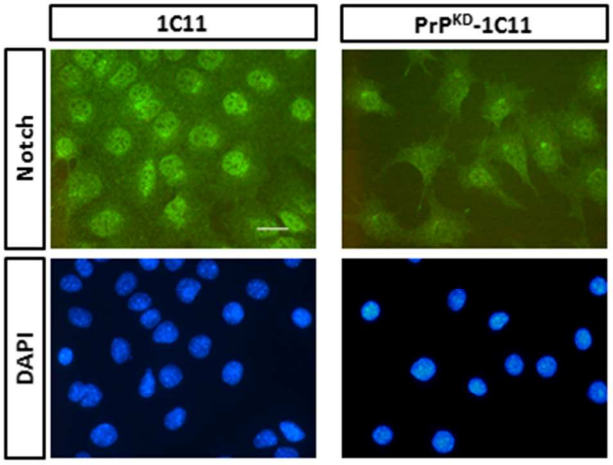

165x119mm (300 x 300 DPI)

S2 Fig

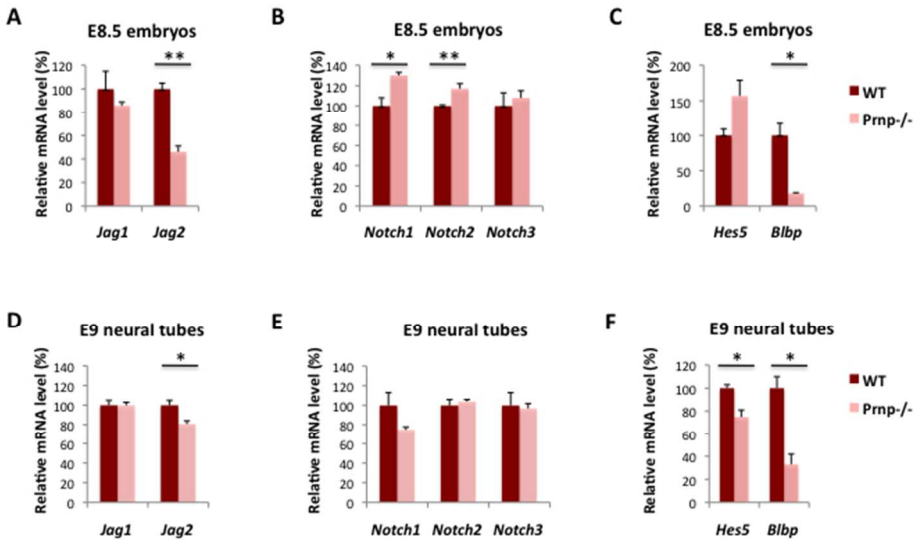

254x190mm (72 x 72 DPI)

S3 Fig

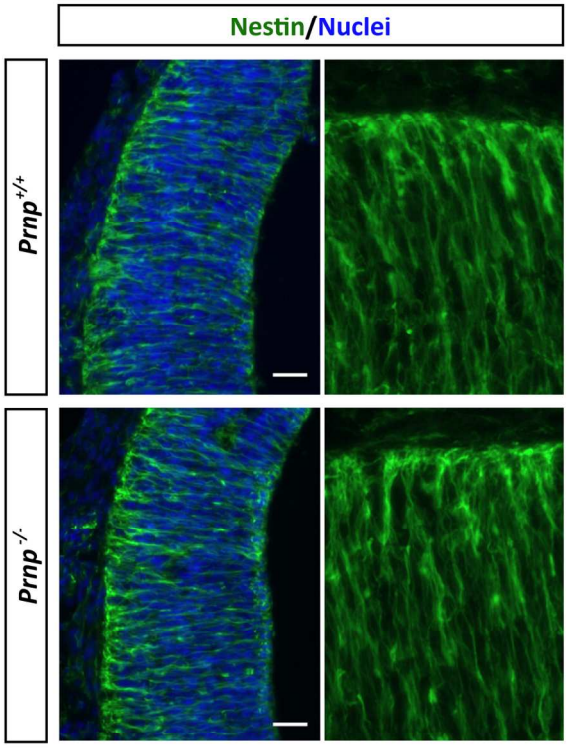

149x137mm (300 x 300 DPI)

S4 Fig

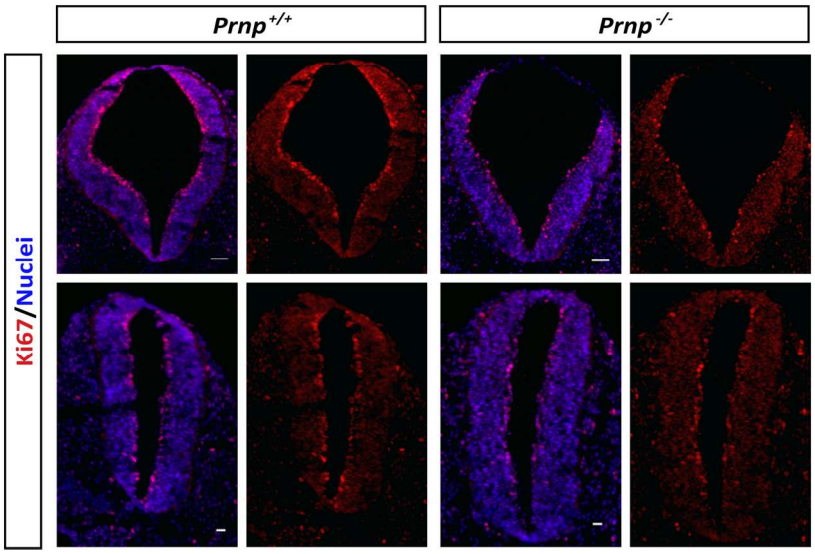

170x115mm (300 x 300 DPI)

S5 Fig

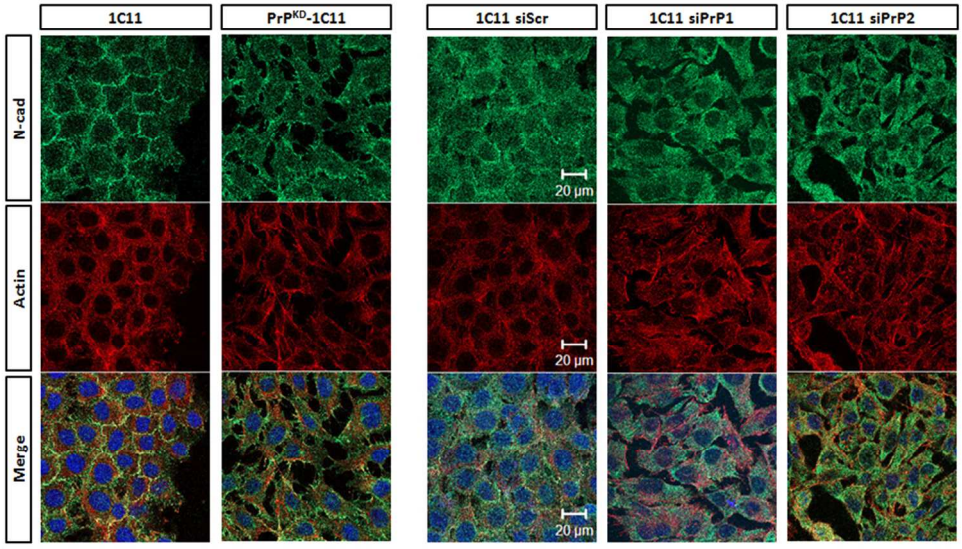

78x50mm (300 x 300 DPI)

S6 Fig

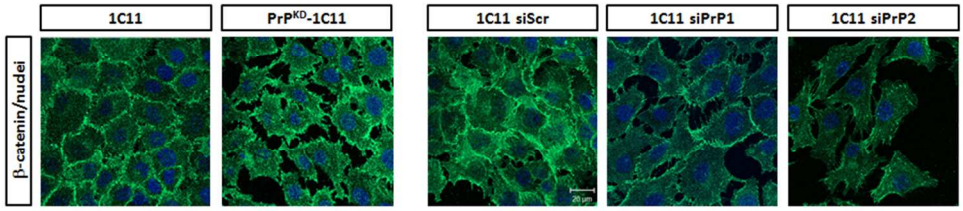

79x29mm (300 x 300 DPI)

S7 Fig

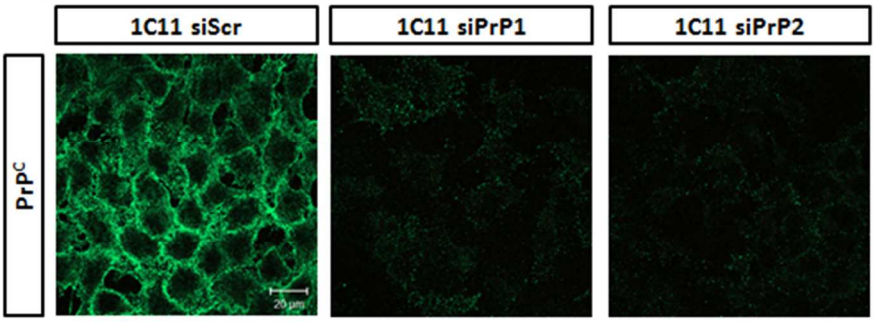

51x20mm (300 x 300 DPI)

S8 Fig

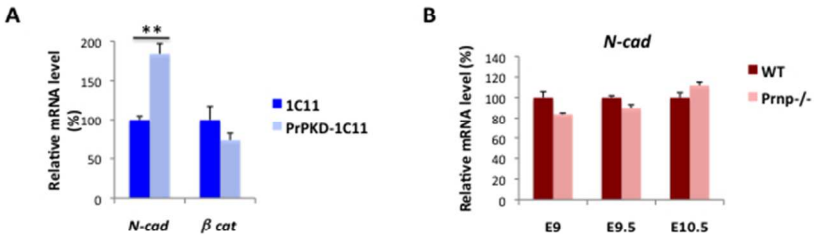

254x190mm (72 x 72 DPI)

S9 Fig

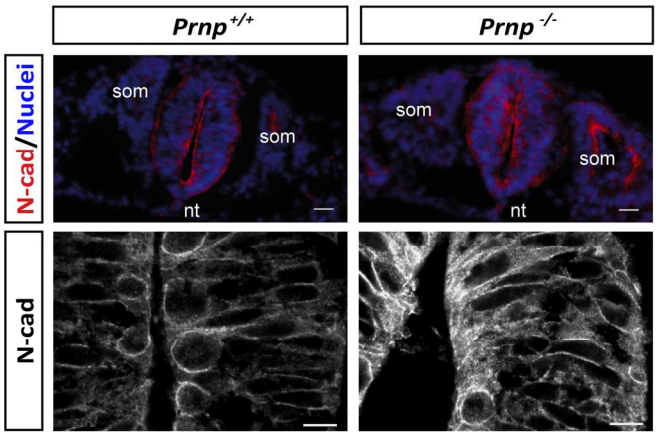

166x108mm (300 x 300 DPI)

S10 Fig

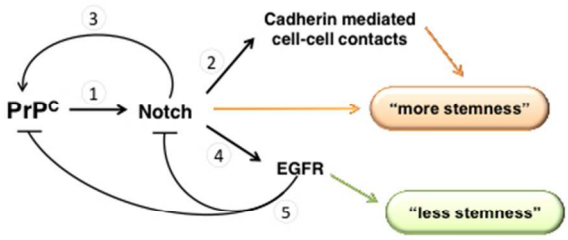

254x190mm (72 x 72 DPI)

Graphical abstract

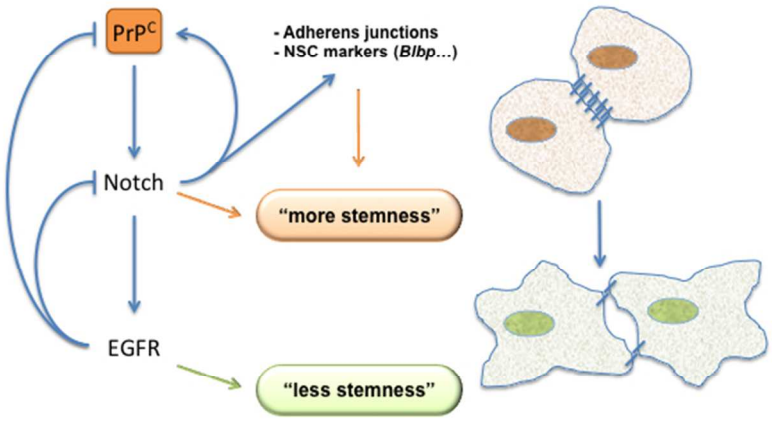

254x190mm (72 x 72 DPI)